

THERMAL ANALYSIS BY ELECTRICAL RESISTIVITY MEASUREMENT

D. D. L. Chung

Composite Materials Research Laboratory, University at Buffalo, The State University of New York, New York 14260-4400, USA

(Received February 5, 2001)

Abstract

Thermal analysis in the form of electrical resistivity measurement is reviewed. It is useful for studying phase transitions and electrical conduction mechanisms. The resistivity can be the volume resistivity or the contact resistivity, as illustrated for the case of continuous carbon fiber polymer-matrix composites.

Keywords: composite, conduction mechanism, electrical resistance, electrical resistivity, phase transition, thermal analysis

Introduction

Thermal analysis refers to the analysis of a material through measurement of a quantity as a function of temperature. The quantity may be heat (as in the case of calorimetry, usually differential scanning calorimetry (DSC) [1–10]), mass (as in the case of thermogravimetry, i.e., thermogravimetric analysis (TG) [11, 12]), dimension (as in the case of dilatometry, i.e., thermomechanical analysis (TMA) [3, 8, 10]), dynamic mechanical properties such as loss tangent and storage modulus (as in the case of dynamic mechanical analysis (DMA), i.e., dynamic thermomechanical analysis (DTMA) [3–6, 9, 10, 12–16]), etc. Thermal analysis can provide information on structural transitions, specific heat, coefficient of thermal expansion (CTE), process kinetics, thermal stability and composition.

A method of thermal analysis which has received relatively little attention involves the measurement of the electrical resistance as a function of temperature. This method requires the material to be electrically conducting. Thus, a polymer which insulates is not suitable for this method. However, polymers containing electrically conducting fillers are conducting and are thus suitable for this method. An example of such a material is a polymer reinforced with carbon fibers, which are conducting and render the composite high strength and high modulus, as required for lightweight structures. Metals, semiconductors and semimetals are also suitable, due to their conductivity.

The measurement of electrical resistance is fast, non-destructive and simple in terms of the equipment, which may be portable. It is thus amenable to process monitoring in real time, even in the field. Measurement of the temperature dependence of the electrical resistivity is also valuable for fundamental study of electrical conduction mechanisms, phase transitions and phonons (such as lattice vibrations).

This paper is a review of thermal analysis conducted by measuring the electrical resistivity as a function of temperature.

Phase transitions

Phase transitions include structural, electrical and magnetic transitions. Examples of structural transitions are the change from one crystal structure to another, the change from an amorphous state to a crystalline state, the glass transition, melting, solidification, cold-crystallization and solid-state curing. Examples of electrical transitions are the change from a metallic state to an insulator state and the change from a normal conducting state to a superconducting state. An example of a magnetic transition is the change from a ferromagnetic state to a paramagnetic state. Phase transitions in general tend to affect the electrical resistivity, thereby allowing resistivity measurements to indicate phase transitions. However, not all phase transitions give rise to a significant change in the electrical resistivity.

Thermal analysis in the form of electrical resistivity measurement has been used in studying phase transitions in metals [17–27], semiconductors [28], C_{60} [29], oxides [30, 31], carbides [32], various compounds [33], composites [34, 35] and other materials. The case of a polymer-matrix composite is described below as an illustration [34, 35].

The polymer matrix of a composite material can undergo structural transitions such as glass transition, melting, cold-crystallization and solid-state curing. Although the polymer matrix is insulating, the effect of a structural transition on the fiber morphology (e.g., the fiber waviness) results in an increase in the volume electrical resistivity of the composite in the fiber direction, thereby allowing the resistance change to indicate a structural transition of the matrix [34, 35].

The glass transition and melting behavior of a thermoplastic polymer depends on the degree of crystallinity, the crystalline perfection and other factors [36–41]. Knowledge of this behavior is valuable for processing and the use of the polymer. This behavior is most commonly studied by DSC [36–41], although the DSC technique is limited to small samples and the associated equipment is expensive and not portable. As the degree of crystallinity and the crystalline perfection of a polymer depend on the prior processing of the polymer and the effect of a process on the microstructure depends on the size and geometry of the polymer specimen, it is desirable to test the actual piece (instead of a small sample) for the glass transition and melting behavior. The measurement of electrical resistance provides a technique for this purpose.

DSC is a thermal analysis technique for recording the heat necessary to establish a zero temperature difference between a substance and a reference material, which

are subjected to identical temperature programs in an environment heated or cooled at a controlled rate [42]. The recorded heat flow gives a measure of the amount of energy absorbed or evolved in a particular physical or chemical transformation. The concept behind the electrical resistance technique is totally different from that of DSC. This technique involves measuring the DC electrical resistance when the polymer has been reinforced with electrically conducting fibers such as continuous carbon fibers. The resistance is in the fiber direction. The polymer molecular movements that occur at the glass transition and melting disturb the carbon fibers, which are much more conducting than the polymer matrix, and thus affect the electrical resistance of the composite in the fiber direction, thereby allowing the resistance change to indicate the glass transition and melting behavior.

Exposure of polyamides to heat and oxygen may cause changes in the physical and chemical characteristics due to thermal oxidative degradation [43] and thus changes in the mechanical properties. Prolonged annealing at a high temperature results in undesirable changes in the degree of crystallization and in the end groups, and may cause inter- and intramolecular transamidation reactions, chain scission and crosslinking [44–49]. The electrical resistance technique is capable of studying the effect of annealing (in air at various temperatures below the melting temperature for various lengths of time) on the glass transition and melting behavior.

Table 1 Calorimetry data for Nylon-6/CF composite before and after annealing

Designation	Annealing condition		$T_m^a/$	$T_{onset}^b/$	$T_m^c/$	$\Delta H^{**}/$
	Temperature/°C	Time/h				
a	*	*	–	200.9	218.5	26.7
b	100	5	–	205.5	218.2	26.6
c	180	5	194.8	201.3	215.5	34.8
d	180	15	196.3	201.4	208.9	39.1
e	180	30	196.3	200.0	209.0	38.6
f	200	5	208.3	212.9	216.4	16.5

^aPeak temperature of the low-temperature melting peak

^bOnset temperature of the high-temperature melting peak

^cPeak temperature of the high-temperature melting peak

** Heat of fusion

* As received

Figure 1a shows the DSC curve of an as-received continuous carbon fiber Nylon-6 matrix composite. The glass transition was not observed by DSC. T_m (melting temperature, as indicated by the peak temperature) was 218.5°C. Figures 1b–1f show the effect of annealing time and temperature on the melting peak. The DSC results are summarized in Table 1 [34]. Since T_m and ΔH of as-received and 100°C (5 h) annealed samples were almost the same (Figs 1a and 1b), it was attributed to the little change of the crystal perfection or the degree of crystallinity during annealing at 100°C for 5 h. Figure 1c shows the DSC curve of the sample annealed at 180°C for 5 h.

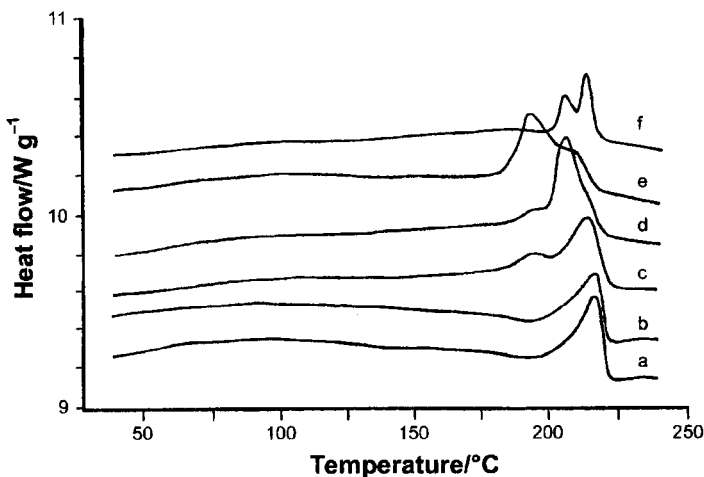


Fig. 1 DSC curves showing the melting endothermic peaks before and after annealing at the temperatures and for the times shown; a – as-received; b – 100°C, 5 h; c – 180°C, 5 h; d – 180°C, 15 h; e – 180°C, 30 h; f – 200°C, 5 h

5 h. It reveals two endothermic melting peaks with peak temperatures of 216 and 195°C. The lower temperature peak may be because of the structural reorganization during annealing, in which the amorphous portion partly developed crystallinity [24, 37, 38]. As the annealing time increased to 15 h (Fig. 1d), the high-temperature peak shifted to a lower temperature, but ΔH increased. As the annealing time increases to 30 h (Fig. 1e), the area of the low-temperature peak increased while that of the high-temperature peak decreased. These effects are probably due to the reorganization and thermal oxidative degradation of the Nylon-6 matrix, as explained below. When the annealing time increased from 5 h (Fig. 1c) to 15 h (Fig. 1d), the degree of the crystallinity increased, so ΔH increased. However, at the same time, the extent of degradation increased due to thermal oxidation, which occurred during annealing at a high-temperature (180°C), thus resulting in lower crystal perfection. Therefore, the high-temperature peak shifted to a lower temperature. When the annealing time was long enough (30 h, Fig. 1e), the crystalline portion from the reorganization process became dominant, as indicated by the increase of the area of the low-temperature peak. When the sample had been annealed at 200°C for 5 h (Fig. 1f), both T_m and ΔH decreased relative to the as-received sample. One possible explanation is that, when the annealing temperature was very high, the extent of thermal degradation was extensive, resulting in less crystalline perfection as well as a lower degree of crystallinity.

Figure 2a [34] shows the fractional change in resistance for the as-received carbon fiber Nylon-6-matrix composite during heating, in which the temperature was raised from 25 to 350°C at a rate of 0.5°C min⁻¹. Two peaks were observed. The onset temperature of the first peak was 80°C and that of the second peak was 220°C. The

first peak is attributed to matrix molecular movement above T_g ; the second peak is attributed to matrix molecular movement above T_m . Because the molecular movement above T_g is less drastic than that above T_m , the first peak is much lower than the second one. As indicated before, the DSC curve of the as-received composite does not show a clear glass transition (Fig. 1a). Therefore, the resistance is more sensitive to the glass transition than DSC. The onset temperature (220°C) of the second peak (Fig. 2a) is higher than the onset temperature ($T_{\text{onset}}=200.9^\circ\text{C}$) of the DSC melting peak (Fig. 1a) and is close to the melting temperature ($T_m=218.5^\circ\text{C}$) indicated by DSC (Fig. 1a). The matrix molecular movement at T_{onset} is less intense than that at T_m , thereby giving no effect on the resistance curve at T_{onset} . Another reason may be a time lag between the matrix molecular movement and the resistance change.

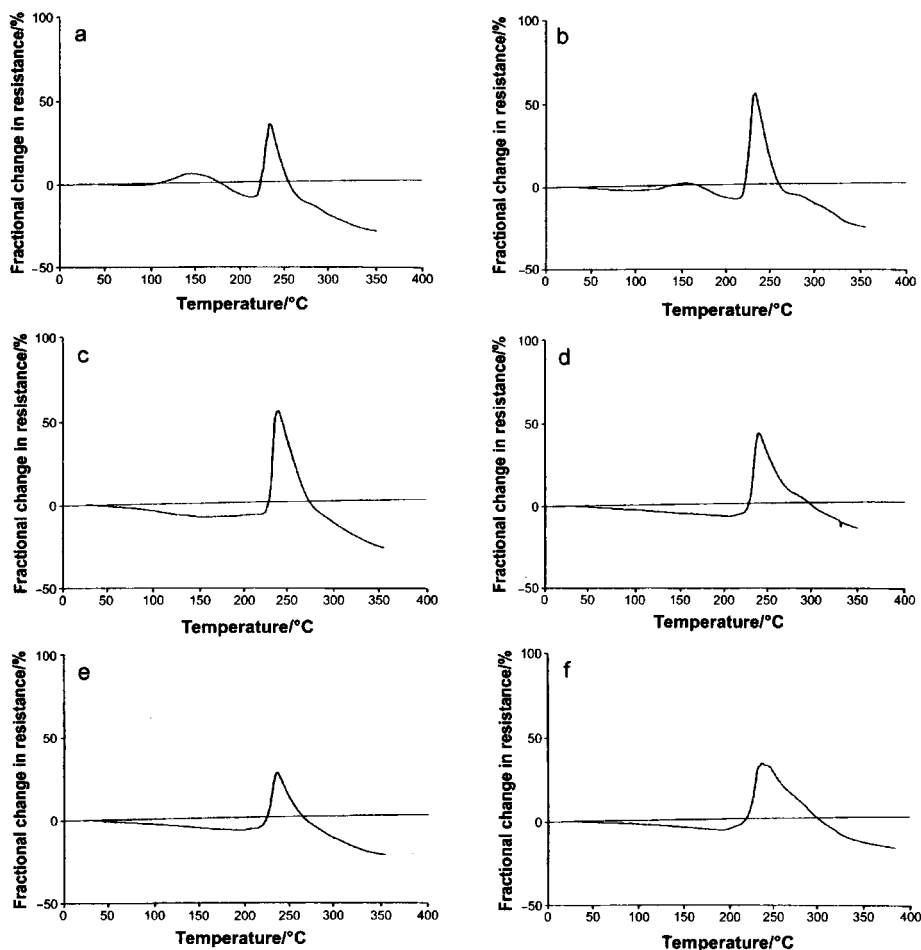


Fig. 2 Effect of annealing condition on the variation of the electrical resistance with temperature; a – as-received; b – 100°C , 5 h; c – 180°C , 5 h; d – 200°C , 5 h; e – 180°C , 15 h; f – 180°C , 30 h

Figures 2b–2d show the effect of the annealing temperature. Comparison of Figs 2a and 2b show that annealing at 100°C for 5 h (Fig. 2b) had little effect on the glass transition and melting behavior of the Nylon-6 matrix; this is consistent with the DSC results (Figs 1a and 1b). When the annealing temperature increased to 180°C (Fig. 2c), the peak due to molecular movement above T_g disappeared. This is attributed to the increase of the degree of crystallinity due to annealing. Because the crystalline portion has constraint on the molecule mobility, the higher the degree of crystallinity, the less is the possibility of molecular movement above T_g .

Not only does the degree of crystallinity but also the extent of thermal degradation affects the molecular mobility above T_g . Figure 2d shows the fractional change in resistance of the sample annealed at 200°C for 5 h. No peak due to molecular movement above T_g was observed. The degree of crystallinity was less than that of the as-received sample, as shown by ΔH in Table 1. However the higher extent of thermal degradation resulted in less molecular movement above T_g .

Figures 2c and 2e show the effect of annealing time from 5 to 15 h at 180°C. The height of the peak due to molecular movement above T_m decreased as the annealing time increased. A longer annealing time resulted in more thermal degradation of the matrix, which retarded the molecular movement above T_m . This effect due to a change of the extent of thermal degradation is also supported by the effect of annealing temperature, as shown in Figs 2c and 2d. A higher annealing temperature is likely to enhance the extent of thermal degradation, thus resulting in a decrease of the height of the peak associated with molecular movement above T_m . Since the tail is more pronounced for samples with a larger extent of thermal degradation, as shown in Figs 2d and 2f, it may be attributed to the lower molecular mobility due to extensive thermal degradation.

Conduction mechanisms

Metals are characterized by their electrical resistivity increasing with increasing temperature, due to the interaction of charge carriers with phonons. However, semiconductors are characterized by their electrical resistivity decreasing with increasing temperature, due to the charge carriers increasing in concentration with temperature. When the carrier excitation or movement requires the overcoming of an activation energy, the number of movable carriers increases exponentially with increasing temperature. As a consequence, the conductivity increases exponentially with temperature. From the slope of the Arrhenius plot of the log conductivity vs. inverse absolute temperature, the activation energy can be determined.

Thermal analysis in the form of electrical resistivity measurement has been used in the study of conduction mechanisms in metals [50–55], semiconductors [56, 57], silicides [58, 59], germanides [60], carbon-nitrogen [61], carbides [62], oxides [63], composites [64–67] and other materials. The case of a continuous carbon fiber polymer-matrix composite is described below as an illustration [66, 67].

The study of the interlaminar interface in a composite laminate is commonly performed by measuring the interlaminar shear strength (ILSS) by techniques such as

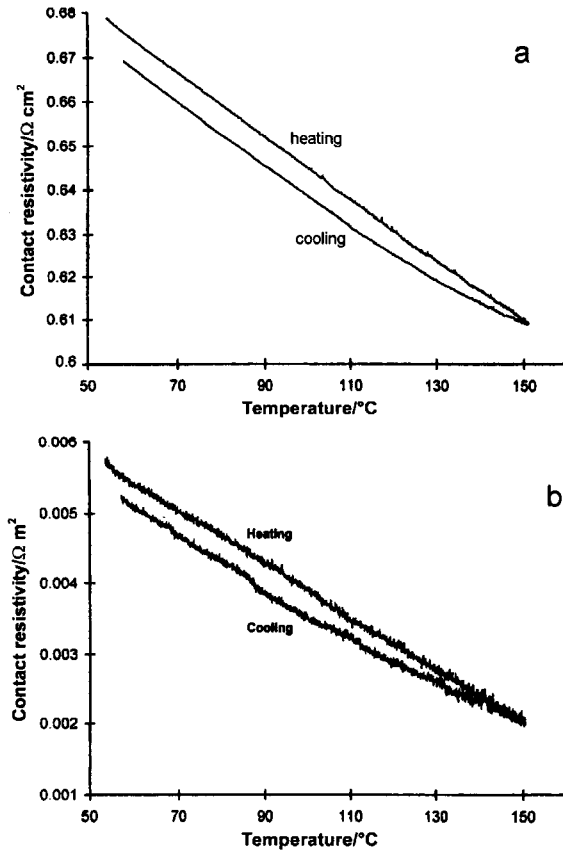


Fig. 3 Variation of contact electrical resistivity with temperature during heating and cooling at $0.15^\circ\text{C min}^{-1}$ a – for sample made without any curing pressure and b – for sample made with a curing pressure 0.33 MPa

the short-beam method [68], the Iospiescu method [69] and other methods [70]. Although ILSS is a valuable quantity that describes the mechanical property of the joint between laminae, it gives little information on the interfacial structure, such as the extent of direct contact (with essentially no polymer matrix in between) between fibers of adjacent laminae and the residual interlaminar stress resulting from the anisotropy between adjacent laminae. The anisotropy is severe when the fibers in the adjacent laminae are in different directions, since the fibers and polymer matrix differ greatly in modulus and thermal expansion coefficient. Direct contact between fibers of adjacent laminae occurs due to the flow of the matrix during composite fabrication and the waviness of the fibers. Direct contact means that the thickness of the matrix between the adjacent fibers is so small (a few Å) that electrons can tunnel or hop from one fiber to the other. The presence of direct contact has been shown by the fact that the volume electrical resistivity of carbon fiber epoxy-matrix composites in the

through-thickness direction is finite, even though the epoxy matrix is electrically insulating [71].

The contact electrical resistivity of the interlaminar interface can be used as a quantity to describe the structure of this interface [66, 67]. Figure 3 shows the variation of the contact resistivity ρ_c with temperature during reheating and subsequent cooling, both at $0.15^\circ\text{C min}^{-1}$, for samples cured at 0 and 0.33 MPa. The corresponding Arrhenius plots of log contact conductivity (inverse of contact resistivity) vs. inverse absolute temperature during heating are shown in Fig. 4. From the slope (negative) of the Arrhenius plot, which is quite linear (not completely linear, probably due to the effect of temperature on the microstructure), the activation energy can be calculated by using the equation

$$\text{slope} = -\frac{E}{23k} \quad (1)$$

where k is the Boltzmann's constant, T is the absolute temperature (in K), and E is the activation energy. The linearity of the Arrhenius plot means that the activation energy does not change throughout the temperature variation. This activation energy is the energy for electron jumping from one lamina to the other. Electronic excitation across this energy enables conduction in the through-thickness direction. This activation phenomenon is common in the electrical conduction of composite materials with an insulating matrix and an electrically conducting filler (whether particles or fibres). Based on volume resistivity measurement, an activation energy in the range from 0.060 to 0.069 eV has been previously reported for short carbon fiber polymer-matrix composites [72]. Direct measurement of the contact resistivity is impossible for the short fiber composites.

The activation energies, thicknesses and room temperature contact resistivity for samples made at different curing pressures and composite configurations are shown in Table 2. As for the same composite configuration (crossply), the higher is the curing pressure, the smaller is the composite thickness (because of more epoxy being squeezed out), the lower is the contact resistivity, and the higher is the activation energy. A smaller composite thickness corresponds to a higher fiber volume fraction in the composite. During curing and subsequent cooling, the matrix shrinks while the carbon fibers essentially do not, so a longitudinal compressive stress will develop in the fibers. For carbon fibers, the modulus in the longitudinal direction is much higher than that in the transverse direction. Thus, the overall shrinkage in the longitudinal direction tends to be less than that in the transverse direction. Therefore, there will be a residual interlaminar stress in the two crossply layers in a given direction. This stress accentuates the barrier for the electrons to jump from one lamina to the other. The greater the residual interlaminar stress, the higher the barrier, which is the activation energy. After curing and subsequent cooling, heating will decrease the thermal stress, due to the CTE mismatch between fibers and matrix. Both the thermal stress and the curing stress contribute to the residual interlaminar stress. Therefore, the higher the curing pressure, the larger the fiber volume fraction, the greater the residual interlaminar stress, and the higher the activation energy, as shown in Table 2. Most of the

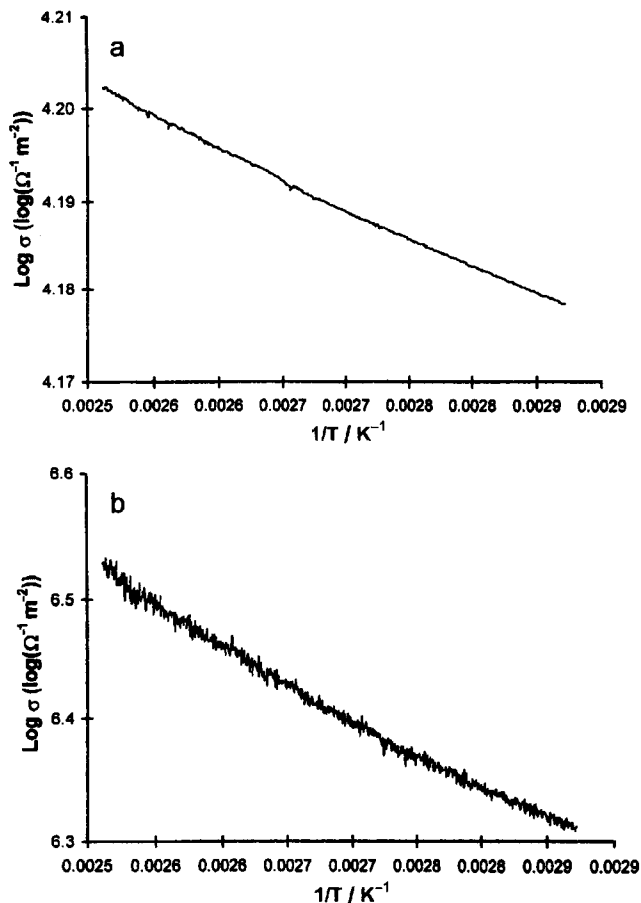


Fig. 4 Arrhenius plot of logarithmic contact conductivity vs. inverse absolute temperature during heating at $0.15^{\circ}\text{C min}^{-1}$ a – for sample made without any curing pressure and b – for sample made with curing pressure 0.33 MPa

values of the activation energy shown in Table 2 are less than kT (where k is the Boltzmann's constant and T is the absolute temperature). This means that the electron jumping from one lamina to the other occurs with ease.

The curing pressure for the sample in the unidirectional composite configuration is higher than that of any of the crossply samples (Table 2). Consequently, the thickness is the lowest. As a result, the fiber volume fraction is the highest. However, the contact resistivity of the unidirectional sample is the second highest rather than being the lowest, and its activation energy is the lowest rather than the highest. The low activation energy is consistent with the fact that there is no CTE or curing shrinkage mismatch between the two unidirectional laminae and, as a result, no interlaminar stress between the laminae. This low value supports the notion that the interlaminar stress is important in affecting the activation energy. The high contact resistivity for

Table 2 Activation energy for various composites. The standard deviations are shown in parentheses

Composite configuration	Curing pressure/MPa	Composite thickness/mm	Contact resistivity, $\rho_{cs}/\Omega \text{ cm}^2$	Activation energy/eV		
				heating at $0.15^\circ\text{C min}^{-1}$	heating at 1°C min^{-1}	cooling at $0.15^\circ\text{C min}^{-1}$
Crossply	0	0.36	0.73	0.0131 ($2 \cdot 10^{-5}$)	0.0129 ($3 \cdot 10^{-5}$)	0.0125 ($8 \cdot 10^{-6}$)
	0.062	0.32	0.14	0.0131 ($4 \cdot 10^{-5}$)	0.0127 ($7 \cdot 10^{-5}$)	0.0127 ($4 \cdot 10^{-5}$)
	0.013	0.31	0.18	0.0168 ($3 \cdot 10^{-5}$)	0.0163 ($4 \cdot 10^{-5}$)	0.0161 ($2 \cdot 10^{-5}$)
	0.19	0.29	0.054	0.0222 ($3 \cdot 10^{-5}$)	0.0223 ($3 \cdot 10^{-5}$)	0.0221 ($1 \cdot 10^{-5}$)
	0.33	0.26	0.0040	0.118 ($4 \cdot 10^{-4}$)	0.129 ($8 \cdot 10^{-4}$)	0.117 ($3 \cdot 10^{-4}$)
	0.42	0.23	0.29	0.0106 ($3 \cdot 10^{-5}$)	0.0085 ($4 \cdot 10^{-5}$)	0.0081 ($2 \cdot 10^{-5}$)
Unidirectional						

the unidirectional case can be explained in the following way. In the crossply samples, the pressure during curing forces the fibers of the two laminae to press on to one another and hence contact tightly. In the unidirectional sample, the fibers of one of the laminae just sink into the other lamina at the junction, so pressure helps relatively little in the contact between fibers of adjacent laminae. Moreover, in the crossply situation, every fiber at the lamina-lamina interface contacts many fibers of the other lamina, while, in the unidirectional situation, every fiber has little chance to contact the fibers of the other lamina. Therefore, the number of contact points between the two laminae is less for the unidirectional sample than the crossply samples.

Conclusions

Thermal analysis in the form of electrical resistivity measurement is useful for studying phase transitions and electrical conduction mechanisms of electrical conductors, including metals, semiconductors, ceramics, carbons and composite materials. The technique is applicable to large specimens and involves simple and portable equipment. The resistivity measured can be the volume resistivity or the contact resistivity, as illustrated for the case of continuous carbon fiber polymer-matrix composites.

References

- 1 J. Mijovic and T. C. Gsell, *SAMPE Quarterly-Society for the Advancement of Materials and Process Engineering*, 21 (1990) 42.
- 2 K. C. Cole, D. Noel, J.-J. Hechler, A. Chouliotis and K. C. Overbury, *Polymer Composites*, 10 (1989) 150.
- 3 W.-D. Emmerich and E. Kaisersberger, in *Materials Science Monographs*, Vol. 35, Elsevier, Amsterdam p. 289.
- 4 W. J. Sichina and P. S. Gill, in *Tech. Sessions of the 41st Annual Conf., – Reinforced Plastics/Composites Institute, SPI, New York 1986, Sess. 24, 4 p.*
- 5 J. N. Leckenby, D. C. Harget, W. J. Sichina and P. S. Gill, in *Carbon Fibers: Technology, Uses and Prospects*, Noyes Publ., Park Ridge, NJ, 1985, p. 86.
- 6 J. N. Leckenby, D. C. Harget, W. J. Sichina and P. S. Gill, in *Carbon Fibers III, Plastics and Rubber Inst., London 1985, p. 111.*
- 7 T. W. Johnson and C. L. Ryan, in *Proc. 31st International SAMPE Symposium and Exhibition 1986: Materials Sciences for the Future, SAMPE, Azusa, CA, 1986, p. 1537.*
- 8 D. Wong, J. Jankowsky, M. DiBerardino and R. Cochran, in *Proc. 38th Int. SAMPE Symp. and Exhibition, SAMPE, Covina, CA, Part 2, 38 (1993) 1552.*
- 9 K. E. Atkinson and C. Jones, *J. Adhesion*, 56 (1996) 247.
- 10 J. L. Jankowsky, D. G. Wong, M. F. DiBerardino and R. C. Cochran, in *ASTM Special Technical Publication, No. 1249, Proc. Symp. on Assignment of the Glass Transition, ASTM, Philadelphia, PA, 1994, p. 277.*
- 11 P. Olivier, J. P. Cottu and B. Ferret, *Composites*, 26 (1995) 509.
- 12 A. Licea-Claverie and F. J. U. Carrillo, *Polymer Testing*, 16 (1997) 445.

- 13 B. Harris, O. G. Graddell, D. P. Almond, C. Lefebvre and J. Verbist, *J. Mater. Sci.*, 28 (1993) 3353.
- 14 M. Akay, J. G. Cracknell and H. A. Farnham, *Polymers and Polymer Composites*, 2 (1994) 317.
- 15 J. W. E. Gearing and M. R. Stone, *Polymer Composites*, 5 (1984) 312.
- 16 J. R. Sarasua and J. Pouyet, *J. Thermoplastic Composite Materials*, 11 (1998) 2.
- 17 T. Fukuda, T. Kakeshita, T. Saburi, K. Kindo, T. Takeuchi, M. Honda and Y. Miyako, *Physica B: Condensed Matter*, 237-238 (1997) 609.
- 18 M. Kato, Y. Nishino, S. Asano and S. O'Hara, *Nippon Kinzoku Gakkaishi/J. Japan Inst. of Metals*, 62 (1998) 669.
- 19 N. Afify, A. Gaber, M. S. Mostafa and A. A. Hussein, *J. Alloys and Compounds*, 259 (1997) 135.
- 20 M. Bizjak and L. Kosec, *Zeitschrift für Metallkunde*, 91 (2000) 160.
- 21 P. Archambault and D. Godard, *Scripta Materialia*, 42 (2000) 675.
- 22 U. Schmidt, C. Eisenschmidt, T. Vieweger, C. Y. Zahra and A.-M. Zahra, *J. Non-Crystalline Solids*, 271 (2000) 29.
- 23 Y. S. Kwon and B. H. Min, *Physica B: Condensed Matter*, 281 (2000) 120.
- 24 M. Hedo, T. Nakama, A. T. Burkov, K. Yagasaki, Y. Uwatoko, H. Takahashi, T. Nakanishi and N. Mori, *Physica B: Condensed Matter*, 281 (2000) 88.
- 25 H. Kadomatsu, K. Kuwano, K. Umeo, Y. Itoh and T. Tokunaga, *J. Magnetism and Magnetic Mater.*, 189 (1998) 341.
- 26 Y. Karaki, M. Kubota, H. Ishimoto and Y. Onuki, *Physica B: Condensed Matter*, 284 (2000) 1690.
- 27 R. Troc, V. Zaremba, M. Kuznietz and E. M. Levin, *J. Alloys and Compounds*, 297 (2000) 9.
- 28 E. M. Levin, V. K. Pecharsky, K. A. Gschneidner Jr. and P. Tomlinson, *J. Magnetism and Magnetic Mater.*, 210 (2000) 181.
- 29 S. Rogge, A. W. Dunn, T. Melin, C. Dekker and L. J. Geerligs, *Carbon*, 38 (2000) 1647.
- 30 V. G. Orlov, A. A. Bush, S. A. Ivanov and V. V. Zhurov, *J. Low Temp. Physics*, 105 (1996) 1541.
- 31 S. Fujihara, G. Murakami and T. Kimura, *J. Alloys and Compounds*, 243 (1996) 70.
- 32 D. Lipp, A. Gladun, K. Bartkowski, A. Belger, P. Paufler and G. Behr, *Physica B: Condensed Matter*, 284 (2000) 1103.
- 33 M. M. Abdel-Kader, M. M. Mosaad, M. A. Fahim, K. K. Tahoon and Z.H. El-Tanahy, *Phase Transitions*, 62 (1997) 105.
- 34 Z. Mei and D. D. L. Chung, *Polymer Composites*, 21 (2000) 711.
- 35 Z. Mei and D. D. L. Chung, *Polymer Composites*, 19 (1998) 709.
- 36 J. A. Kuphal, L. H. Sperling and L. M. Robeson, *J. Appl. Polym. Sci.*, 42 (1991) 1525.
- 37 A. L. Simal and A. R. Martin, *J. Appl. Polym. Sci.*, 68 (1998) 453.
- 38 Ch. R. Davis, *J. Appl. Polym. Sci.*, 62 (1996) 2237.
- 39 B. G. Risch and G. L. Wilkes, *Polymer*, 34 (1993) 2330.
- 40 H. J. Oswald, E. A. Turi, P. J. Harget and Y. P. Khanna, *J. Macromol. Sci. Phys.*, B13 (1977) 231.
- 41 J. U. Otaigbe and W. G. Harland, *J. Appl. Polym. Sci.*, 36 (1988) 165.
- 42 M. E. Brown in *Introduction to Thermal Analysis: Techniques and Application*, Chapman and Hall, New York 1988, p. 25.

- 43 C. H. Do, E. M. Pearce and B. J. Bulkin, *J. Polym. Sci., Part A: Polym. Chem.*, 25 (1987) 2409.
- 44 M. C. Gupta and S. G. Viswanath, *J. Thermal Anal.*, 47 (1996) 1081.
- 45 N. Avramova, *Polym. and Polym. Comp.*, 1 (1993) 261.
- 46 A. L. Simal and A. R. Martin, *J. Appl. Polym. Sci.*, 68 (1998) 441.
- 47 I. M. Fouda, M. M. El-Tonsy, F. M. Metawe, H. M. Hosny and K. H. Easawi, *Polym. Testing*, 17 (1998) 461.
- 48 I. M. Fouda, E. A. Seisa and K. A. El-Farahaty, *Polym. Testing*, 15 (1996) 3.
- 49 L. M. Yarisheva, L. Yu. Kabal'nova, A. A. Pedy and A. L. Volynskii, *J. Thermal Anal.*, 38 (1992) 1293.
- 50 Y. Nishino, *Mater. Sci. and Eng. A: Structural Mater.: Properties, Microstructure and Processing*, 1-2 (1998) 50.
- 51 T. Ikeda, T. Miyashita, T. Hirai, M. Ikeda and S. Komatsu, *Keikinzoku/J. Japan Inst. Light Metals*, 49 (1999) 476.
- 52 J. Ivkov and N. Radic, *Solid State Communications*, 106 (1998) 273.
- 53 S. Nishigori, Y. Yamada, T. Ito, H. Abe and A. Matsushita, *Physica B: Condensed Matter*, 281 (2000) 686.
- 54 J. Ederth, L. B. Kiss, G. A. Niklasson, C. G. Granqvist and E. Olsson, *Mater. Res. Soc. Symp. Proc.*, 581 (2000) 541.
- 55 V. D. Das and P. G. Ganesan, *Solid State Communications*, 106 (1998) 315.
- 56 Z. Bendekovic, P. Biljanovic and D. Grgec, in *Proc. 9th Mediterranean Electrotechnical Conf., MELECON, IEEE, Piscataway, N.J.*, 1 (1998) 362.
- 57 V. D. Das and P. G. Ganesan, in *Proc. SPIE – The Int. Soc. Optical Eng., SPIE, Bellingham, WA*, 3316 (1998) 1157.
- 58 S. Majumdar, M. M. Kumar, R. Mallik and E. V. Sampathkumaran, *Solid State Communications*, 110 (1999) 509.
- 59 N. Tateiwa, N. Kimura, T. Sakon, M. Motokawa, H. Aoki and T. Komatsubara, *Physica B: Condensed Matter.*, 281 (2000) 254.
- 60 P. Boulet, F. Weitzer, K. Hiebl and H. Noel, *Physica B: Condensed Matter.*, 292 (2000) 302.
- 61 R. Kurt, R. Sanjines and A. Karimi, *Mater. Res. Soc. Symp. Proc.*, 593 (2000) 511.
- 62 W. S. Williams, *Int. J. Refractory and Hard Metals*, 17 (1999) 21.
- 63 H. Shiomi, M. Nakamura and K. Watanabe, *J. Ceramic Soc. Japan, Int. Ed.*, 102 (1994) 288.
- 64 V. Chellappa, Z. W. Chiou and B. Z. Jang, *J. Mater. Sci.*, 30 (1995) 4263.
- 65 V. Chellappa, L. Zhao and B. Z. Jang, in *Proc. SPIE – The Int. Soc. Optical Eng., SPIE, Bellingham, WA*, 2447 (1995) 68.
- 66 S. Wang and D. D. L. Chung, *Composite Interfaces*, 6 (1999) 497.
- 67 S. Wang and D. D. L. Chung, *Composite Interfaces*, 6 (1999) 507.
- 68 ASTM Standard, D 2344-84 (1995) 43.
- 69 G. Zhou, E. R. Green and C. Morrison, *Composites Sci. Tech.*, 55 (1995) 187.
- 70 S. L. Iyer, C. Sivaramkrishnan and C. Young, in *Proc. of 34th International SAMPE Symp. and Exhibition, SAMPE, Covina, CA, 1989. Book 2*, p. 2172.
- 71 X. Wang and D. D. L. Chung, *Polymer Composites*, 18 (1997) 692.
- 72 A. R. Blythe, in *Electrical Properties of Polymers*, Cambridge University Press, 1980.